FICUP
An International Conference on
Urban Physics
B. Beckers, T. Pico, S. Jimenez (Eds.)
Quito – Galápagos, Ecuador, 26 – 30 September 2016

Sparse Matrix Solution for Computing Urban Radiation Exchange

José Pedro Aguerre[1], **Eduardo Fernández**[1], **Gonzalo Besuvievsky**[2], and **Benoit Beckers**[3]

[1]Centro de Cálculo, Universidad de la República, Uruguay
{jpaguerre,eduardof}@fing.edu.uy

[2]Geometry and Graphics Group, Universitat de Girona, Spain
gonzalo@imae.udg.edu

[3]Roberval Laboratory, Urban Systems Engineering, Universite de Technologie de Compiegne - Sorbonne University, France
benoit.beckers@utc.fr

Keywords: Urban Radiation Exchange, Radiosity, Form Factors, Sparse Matrix, Daylighting

Abstract. *Numerical simulation of cities generates highly complex computational challenges. Many existing computer models should be adapted to consider the physical and social phenomena that are developed in urban environments. In this paper, a numerical model for urban radiation exchanges is analyzed. In this way, the sparsity of the form factors matrix is studied. This matrix is used to solve problems of radiation exchange (light and heat). It is found that this matrix is usually highly sparse, which enables it to be stored in main memory for models up to 140k patches. A technique is also proposed to estimate the inverse of the radiosity matrix, useful for finding radiation exchange. In this calculation, near-zero elements are removed, leading to a highly sparse approximation. These techniques could be useful for the design of buildings, taking into consideration the characteristics of the surroundings, as well as to help in the definition of city regulations related to urban construction.*

1 Introduction

Due to the increasing need of energy assessment tools at large scale, urban physics simulation has become a major topic of interest. This work focuses on light exchange at urban scale. Thermal radiation is not considered in this paper. The evaluation of annual solar irradiance and the analysis of the spatial variation over building facades has a relevant interest for urban planning and building design. Computational simulation for radiative transfer on an urban scale, where thousands of buildings have to be considered, is a challenge. The main problem is how to deal with the huge amount of data required to represent such models.

One of the mathematical models adapted to predict urban radiation exchange is the use of the radiosity method [Cohen and Wallace, 2012; Beckers, 2013a]. A full solution of this method in a city model may require computing the view factors between all building mesh elements and solving the linear system, which may be an expensive computational task considering a district model domain composed of hundred of buildings. A possible solution to manage the problem is to rough simplify the visibility problem [Robinson and Stone, 2005].

We focus on solving the problem considering all visibility information. By observing that the form factor matrix that represents all view factors is generally sparse for this kind of environments, we propose a novel approach for radiative exchange computation that can approximate the inverse of the radiosity matrix. We formulate the problem as a Neumann series and approximate the matrix by eliminating unimportant terms. Our resulted study on different kinds of urban model configuration shows that, for models composed of thousands of patches, we can provide an accurate approximation of the inverse radiosity matrix that can also be stored in main memory. In this way, it can be used to solve efficiently annual based radiative simulations. This is a promissory result, concerning its potential use for radiative exchange and analysis.

The rest of the paper is structured in the following way. Sec. 2 describes the radiosity method, as well as the main related works. Sec. 3 presents our proposal for solving the described problem. Next, the experimental analyses are shown in Sec. 4, where several study cases are presented and evaluated. Finally, Sec. 5 is dedicated to the conclusions and main lines of future works.

2 Related work

The two main methodologies for solving the urban radiant exchange problems are ray tracing and radiosity. While the former is widely used in rendering, the radiosity method is more suitable because it was originally developed for heat transfer exchange computation. One of the advantages of using this method is that it can obtain results in the whole scene space, which makes it attractive for urban environment analysis. In the rest of this section, we review the radiosity method and the works related to our approach.

2.1 The Radiosity Problem

The radiosity method [Goral et al., 1984] is a technique which allows to compute global illumination on scenes with Lambertian surfaces. It has been applied in many areas of design and computer animation [Dutre et al., 2006]. The continuous radiosity equation can be discretized through the use of a finite element methodology. The scene is discretized into a set of patches,

leading to express the problem using the following set of linear equations:

$$B_i = E_i + R_i \sum_{j=1...n} B_j \mathbf{F}(i,j) \quad , \quad \forall i \in \{1 \dots n\}$$

This set of linear equations is expressed in a succinct manner in Equation 1.

$$(\mathbf{I} - \mathbf{RF})B = E, \tag{1}$$

where $\mathbf{I}$ is the identity matrix, $\mathbf{R}$ is a diagonal matrix containing the reflectivity index of each patch, B is the radiosity vector to be found, and E is the emission vector. $\mathbf{F}(i,j)$ is a number between 0 and 1 expressing the form factor between patch i and j. This value indicates the fraction of the light power going from one to another. Therefore, the form factor matrix is a $n \times n$ matrix, where n is the number of patches in the scene.

$\mathbf{F}$ can be efficiently computed using the hemi-cube algorithm [Cohen and Greenberg, 1985], but its memory requirements ($O(n^2)$) are often an obstacle when working with big models ($n > 50.000$).

Equation 1 can be solved using several approaches. For example, the operator $\mathbf{M} = (\mathbf{I} - \mathbf{RF})^{-1}$ can be calculated, which represents a global transport operator relating the emitted light with the final radiosity of the scene, $B = \mathbf{M}E$. When $\mathbf{F}$ has a low numerical rank, factorization techniques can be used to efficiently compute an approximation of $\mathbf{M}$ [Fernández, 2009]. On the other hand, $\mathbf{M}$ can also be approximated using iterative methods such as Neumann series ([Kontkanen et al., 2006]).

Another approach is to compute $\mathbf{B}$ by solving the linear system of equations iteratively, using methods such as Jacobi or Gauss-Seidel ([Cohen and Wallace, 2012]). Eq. 2 presents the radiosity resolution using the Jacobi iteration. Each iteration adds the radiosity of a new light bounce to the global radiosity result.

$$B^{(i+1)} = \mathbf{RF}B^{(i)} + E \quad , \quad \text{where } B^{(0)} = E \tag{2}$$

2.2 Neumann Series

Given an Operator $\mathbf{T}$, its Neumann series is a series of the form

$$\sum_{k=0}^{\infty} \mathbf{T}^k$$

The expression $\mathbf{T}^k$ is a mathematical notation that means applying the operator $\mathbf{T}$, k consecutive times. Supposing that $\mathbf{T}$ is a bounded operator and $\mathbf{I}$ the identity operator, if the Neumann series converges, then $(\mathbf{I} - \mathbf{T})$ is invertible and its inverse is the series:

$$(\mathbf{I} - \mathbf{T})^{-1} = \sum_{k=0}^{\infty} \mathbf{T}^k = \mathbf{I} + \mathbf{T} + \mathbf{T}^2 + \mathbf{T}^3 + ...$$

This property can be used to calculate the radiosity ([Cohen and Wallace, 2012]), by computing an approximate to the inverse of $(\mathbf{I} - \mathbf{RF})$ through l iterations:

$$(\mathbf{I} - \mathbf{RF})^{-1} \approx \mathbf{I} + \mathbf{RF} + (\mathbf{RF})^2 + ... + (\mathbf{RF})^l$$

In this series, $(\mathbf{RF})^i$ contains the information of the i^{th} bounce of light between the surfaces in the scene. The main computational cost of this approach is the multiplication of matrices. Thus, if $\mathbf{RF}$ is sufficiently big, the method can be prohibitively expensive.

[Kontkanen et al., 2006] use a variant of this method to compute a global transport operator for radiance calculations. This operator expresses the relationship between the converged and incoming incident lighting. In this process, the matrices are compressed using the following strategy: at each step, all the coefficients below a certain threshold are removed. This results in sparse matrices, which allow to speed up the calculation. The computation is stopped when all the coefficients in $(\mathbf{RF})^i$ are smaller than the threshold.

2.3 Sparse Matrices in Radiosity Problems

A *sparse matrix* is any matrix with enough zeros that it pays to take advantage of them [Wilkinson, 1971]. Generally, using sparse representations allows to save time or memory (usually both) by exploiting the number of zeros. Furthermore, these kind of matrices are applied in problems where the use of full matrices is not possible due to memory restrictions.

The use of sparse matrices in radiosity calculations is still a subject of study. [Gortler et al., 1993] present the Wavelet Radiosity method, which is based on wavelet theory. Expressing the kernel operating in a radiosity function in a wavelet basis leads to a sparse approximation of it. On the other side, [Goel et al., 1991], [Borel et al., 1991] and [Chelle and Andrieu, 1998] solve the radiosity problem using iterative methods (like Gauss-Seidel) taking advantage of the sparsity of the form factors matrix. This property is present in the tested scenes (plant canopies), where there is a high occlusion level between distant polygons.

2.4 Urban Radiative Methods

A previous work for reducing the urban radiosity formulation is the simplified radiosity algorithm (SRA) [Robinson and Stone, 2005]. The basis of the simplification is grouping, for each sky direction, the main obstructions that obscured each surface. Then, for a scene composed of n patches and getting p sky patches, the system matrix can be reduced to a $n \times p$, that can both be inverted or used to solve the system iteratively. This method is embedded in the CitySim package [Robinson et al., 2009], a multi-purpose system for urban models simulation. In [Beckers, 2013b], the idea of using well-known finite element techniques as condensation, is analyzed for being adapted to urban models. In this case, the analysis is done only for longwave radiation.

3 Our Proposal

This section presents the main ideas of the present work, and proposes an algorithm to compute radiosity solutions exploiting the properties of the studied matrices.

3.1 Studying the Sparsity of a City's Form Factors Matrix

The density factor (sparsity) of a matrix is the fraction of non-zero elements over the total number of elements. In the form factor matrices, this factor depends on how many patches are seen from each patch: if patch j sees few patches, then row j of $\mathbf{F}$ has few elements different than zeros, and vice versa. Figure 1 shows two urban scenes where each patch is colored by checking how

many elements are seen from it. For example, the upper elements on the tallest buildings are red while the ones on houses are blue. This result allows to predict that the $\mathbf{F}$ matrix corresponding to a city, where each patch sees few others, is very sparse.

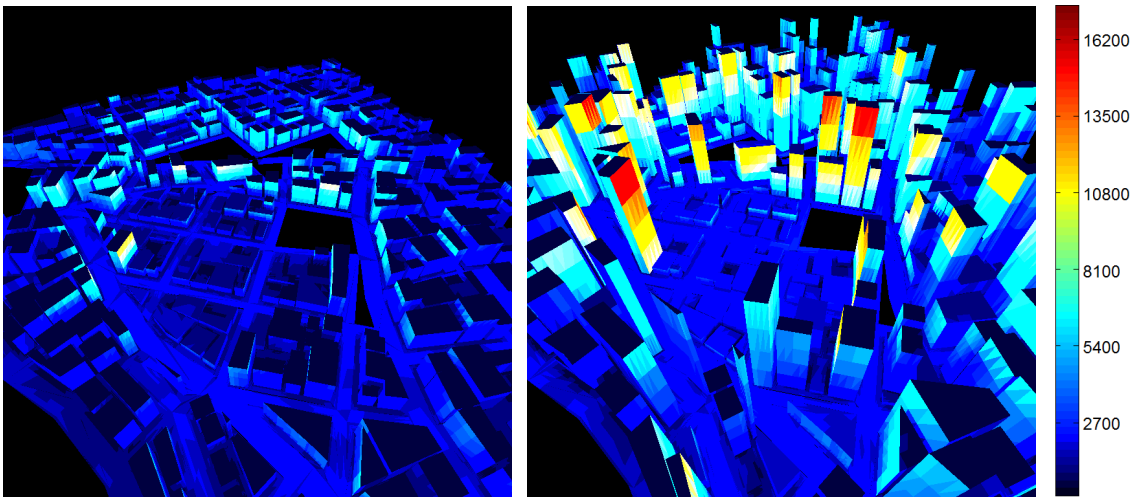

(a) City 1. (b) City 3.

Figure 1: Two example urban scenes. The color of a patch indicates the number of patches that are seen from it.

The previous fact derives into the main conjecture of the present work: different kinds of cities have sparse $\mathbf{F}$ matrices with different density factors. This sparsity depends on many factors. For example, orography, construction type, buildings disposition and heights are expected to have a great influence on the structure of the matrices. In this paper we focus on the variation of building heights. A city with big variance on its buildings height (as a typical contemporary downtown with skyscrapers) should generate less sparse matrices than a city with uniformly elevated buildings (as, for example, Haussmann's Paris).

3.2 An Approximation of $\mathbf{M} = (\mathbf{I} - \mathbf{RF})^{-1}$

The inverse of a sparse matrix is usually a full matrix, where its calculation is computationally expensive, and has memory limitations for medium to large size matrices. However, in the case of the radiosity matrix, its inverse $\mathbf{M}$ has many elements below a small threshold. Therefore, in relation to $\mathbf{M}$, our proposal consists in finding a sparse approximation ($\tilde{\mathbf{M}} \approx \mathbf{M}$) that allows to compute low-error radiosity values.

In order to compute $\tilde{\mathbf{M}}$ efficiently, we use a method based on the work by [Kontkanen et al., 2006]. As described in Sec. 2.2, the algorithm is based on the use of Neumann series and a compression strategy based on removing all elements below a threshold ε. To obtain even sparser matrices, we apply this compression to $\mathbf{RF}$ before starting the process.

Algorithm 1 describes the proposed method, where the function "remove" eliminates $|\mathbf{T}(i,j)| < \varepsilon, \forall i,j$.

$\tilde{\mathbf{M}} = \mathbf{0}$;
$\mathbf{T} = \mathbf{I}$;
while $\mathbf{T} \neq \mathbf{0}$ **do**
  $\tilde{\mathbf{M}} = \tilde{\mathbf{M}} + \mathbf{T}$;
  $\mathbf{T} = \mathbf{T}(\mathbf{RF})$;
  remove$(\mathbf{T}, \varepsilon)$;
end

Algorithm 1: Calculate $\tilde{\mathbf{M}}$.

Once the sparse approximation is computed, it is relatively inexpensive to calculate the radiosity results for k different emissions (Eq. 3):

$$\begin{aligned} \tilde{\mathbf{M}} &\approx (\mathbf{I} - \mathbf{RF})^{-1} \\ \tilde{\mathbf{B}}_k &= \tilde{\mathbf{M}}\mathbf{E}_k \end{aligned} \tag{3}$$

where the i^{th} column of $\mathbf{E}_k$ is an emission and the i^{th} column of $\tilde{\mathbf{B}}_k$ is the approximation of its corresponding radiosity result, $\forall i \in 1 \,..\, k$.

3.3 Daylight Simulation

Computing urban radiation exchange can have increasing interest if it is efficiently calculated. In this work, we apply the described techniques on urban daylight simulation, such kind of simulation has been applied in different fields such as design [Baker and Steemers, 2014], building energy consumption [Hviid et al., 2008] or ecology [Longcore and Rich, 2004].

In order to simulate the sky and its interaction with the city, a hemisphere containing the city is added to the model. This hemisphere is divided into m elements and each element is given its corresponding emittance, simulating the skylight. There are several ways to mesh the sky ([Tregenza, 1987], [Mardaljevic, 1999]), though we use a simple division with parallels and meridians (m=132) as a proof of concept.

Once the sky is added to the model, we use the strategy described at [Beckers, 2013b] to calculate the first bounce of light from the sky in the city. We use this as the urban emission, which allows us to work only with the form factors between patches of the city. For this purpose, Eq. 1 is re-written in the following way:

$$\mathbf{B} = E + \mathbf{RF}B \tag{4}$$

Let us separate sky (index s) and city (index u) contributions in Eq. 4:

$$\begin{bmatrix} B_s \\ B_u \end{bmatrix} = \begin{bmatrix} E_s \\ E_u \end{bmatrix} + \begin{bmatrix} (\mathbf{RF})_{ss} & (\mathbf{RF})_{su} \\ (\mathbf{RF})_{us} & (\mathbf{RF})_{uu} \end{bmatrix} \begin{bmatrix} B_s \\ B_u \end{bmatrix}$$

The sky is considered as a black surface, with zero reflectance, while the city has no emission. Therefore:

$$\begin{bmatrix} B_s \\ B_u \end{bmatrix} = \begin{bmatrix} E_s \\ 0 \end{bmatrix} + \begin{bmatrix} 0 & 0 \\ (\mathbf{RF})_{us} & (\mathbf{RF})_{uu} \end{bmatrix} \begin{bmatrix} B_s \\ B_u \end{bmatrix}$$

In the previous equation, $B_s = E_s$. This leads to the following statement:

$$B_u = (\mathbf{RF})_{us} B_s + (\mathbf{RF})_{uu} B_u = (\mathbf{RF})_{us} E_s + (\mathbf{RF})_{uu} B_u$$

Now, grouping the radiosities from both sides:

$$(\mathbf{I} - (\mathbf{RF})_{uu}) B_u = (\mathbf{RF})_{us} E_s$$

The left side of this equation is the radiosity matrix $(\mathbf{I} - (\mathbf{RF})_{uu})$ times the radiosity result for the city. Therefore, following Eq. 1, the first bounce of light coming from the sky in the city is the new emission $E = (\mathbf{RF})_{us} E_s$.

4 Experimental Analysis

The results of the presented set of experiments were conducted on a desktop computer, with Intel quad-core i7 processor and 16 Gbytes RAM. The calculation of each $\mathbf{F}$ matrix was realized using the hemi-cube technique, where the graphic component was executed on a NVIDIA GeForce-780 GPU processor. The code was implemented on C++, OpenGL, CUDA [Kirk and Hwu, 2010], and MATLAB [MATLAB, 2010].

4.1 Example City Models

The following analysis is performed using three different urban scenes, which are generated from the same cadastral plan. The first model contains only flat houses, the second low and middle-sized buildings, and the third is composed of different sized buildings, including tall skyscrapers. The urban scenes can be observed in Fig. 2

As can be seen, the first model has a small variance on building heights, while the third one has a big variance. The three models are composed of 8897 patches.

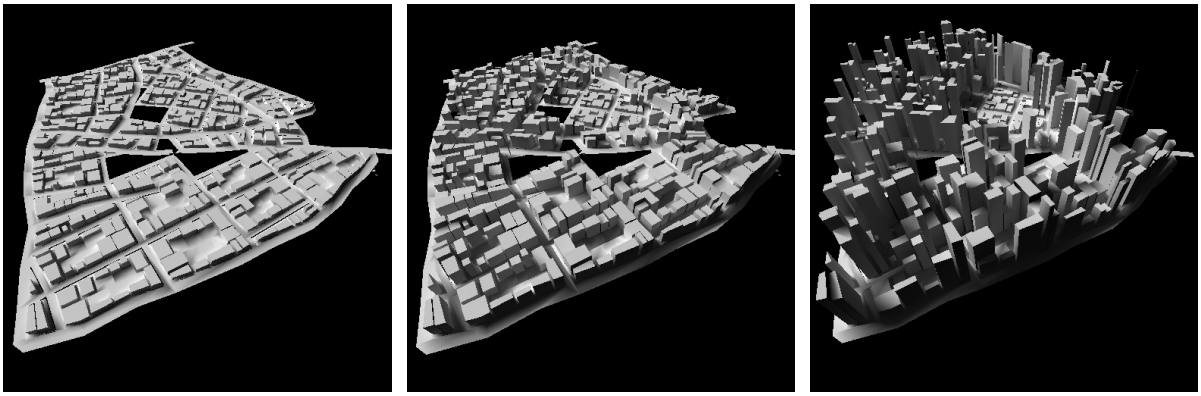

(a) City 1. (b) City 2. (c) City 3.

Figure 2: Three different urban scenes to experiment with.

4.2 Sparsity Results for $\mathbf{F}$ and $\tilde{\mathbf{M}}$

We show the sparsity results for the described city models. For each model, three variants are studied: the original (n=8897), dividing each patch into 4 (n=35588) and into 16 (n=142352), where n is the number of patches. This allows to analyze the proposed algorithm for bigger models, as well as the effect of dividing patches in the sparsity factor. The calculation of $\mathbf{F}$ takes about 20s, 90s, and 600s for n=8897, 35588, and 142352, respectively.

First of all, we explore the density of $\mathbf{M}$ matrices (n=8897, inverted with MATLAB) and the distribution of their elements, for different reflectivity indexes R (Fig. 3). It can be appreciated that most of the matrices elements are non-zero, and also that most of them have very small values. An increment in the value of R is related to an increment in the values of the matrix elements. Finally, the matrices of City 1 have smaller elements than those related to City 3.

In the rest of the paper, a reflectivity index of 0.7 is used. This value is higher than the expected for cities, but it could be useful for challenging the sparsity of the matrices $\tilde{\mathbf{M}}$.

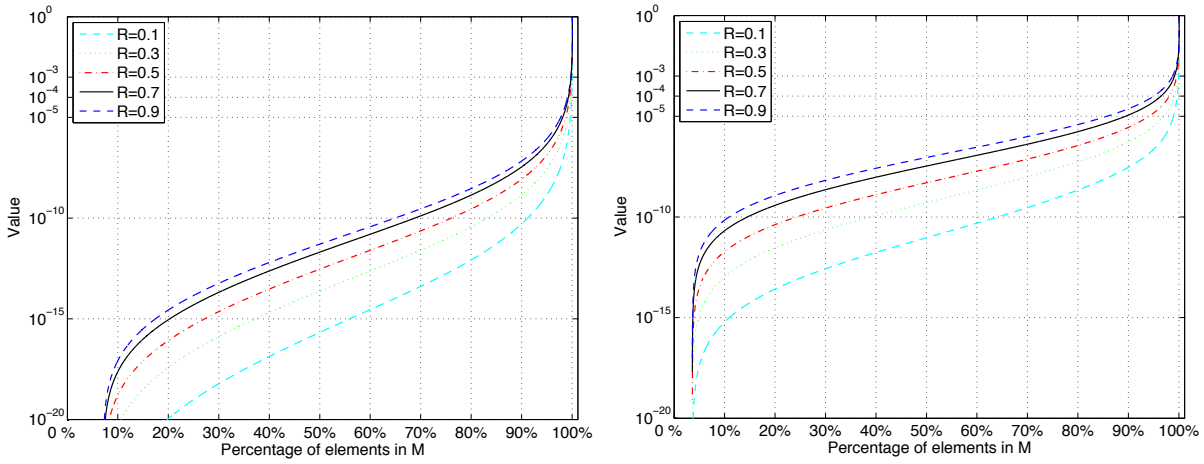

(a) City 1.

(b) City 3.

Figure 3: Distribution function of the $\mathbf{M}$ elements, for different reflectivity indexes and cities.

The sparsity results and memory storage for $\mathbf{F}$ and $\tilde{\mathbf{M}}$ matrices can be seen in Table 1. As expected, the density factor of $\mathbf{F}$ grows as the city model becomes less homogeneous, which implies the use of a larger memory space. Nevertheless, the density reported in the worst case (City 3 with $n = 8897$) signifies a storage of 1.23% of the total elements of the matrix. On the other hand, the density factors are shorter for finer meshes of the same city model.

The density factor of $\tilde{\mathbf{M}}$ has a similar behavior to that described for $\mathbf{F}$. Also, for all cases, the density increases as the threshold ε becomes smaller. The memory required to store the sparse matrices $\mathbf{F}$ and $\tilde{\mathbf{M}}$ is always much less than its full version, for every of the test cases executed.

4.3 Execution Times

In order to study the computational performance of the proposed algorithm, we calculate the daylight illumination for a whole year. For this, we use the 3 city models with the 3 mesh variants,

		Density	Density of $\tilde{\mathbf{M}}$			Memory size (GB)		
	n	of $\mathbf{F}$	$\varepsilon = 10^{-3}$	10^{-4}	10^{-5}	Full	$\mathbf{F}$	$\tilde{\mathbf{M}}$ (10^{-5})
City 1	8897	0.68 %	0.22 %	0.61 %	1.48 %	0.60	0.01	0.02
	35588	0.48 %	0.10 %	0.31 %	0.83 %	9.66	0.09	0.17
	142352	0.35 %	0.04 %	0.15 %	0.45 %	154.60	1.05	1.46
City 2	8897	0.84 %	0.30 %	1.01 %	2.58 %	0.60	0.01	0.03
	35588	0.60 %	0.15 %	0.51 %	1.41 %	9.66	0.12	0.28
	142352	0.44 %	0.05 %	0.24 %	0.75 %	154.60	1.34	2.42
City 3	8897	1.23 %	0.55 %	2.07 %	6.24 %	0.60	0.01	0.08
	35588	0.87 %	0.20 %	0.88 %	2.98 %	9.66	0.17	0.59
	142352	0.64 %	0.06 %	0.36 %	1.40 %	154.60	1.94	4.52

Table 1: Density and memory size of the form factors matrices and the approximated inverse.

along with 3650 sky configurations. The obtained data is compared to the execution times of solving the same radiosity problem iteratively, using the Jacobi iteration (Eq. 2).

Table 2 shows the obtained execution times for the described test cases. The third column shows the speedup over the Jacobi based method. It is important to highlight that this speedup is calculated taking into account both time to compute $\tilde{\mathbf{M}}$ and time to compute $\tilde{\mathbf{M}}\mathbf{E}$. That is: Speedup $= T_J \big/ (T_{\tilde{\mathbf{M}}} + T_{\tilde{\mathbf{M}}\mathbf{E}})$, where T_J is the execution time needed to calculate the radiosity using Jacobi with the same number of iterations (light bounces) than to compute $\tilde{\mathbf{M}}$, for each case.

As can be appreciated in the table, the execution times depend highly on the correspondent density factor of $\tilde{\mathbf{M}}$. The sparsest this matrix is, the lower the execution times are. For the considered example problem, the proposed algorithm works faster than the Jacobi iteration method for all the test cases.

		Time for $\tilde{\mathbf{M}}$ $(T_{\tilde{\mathbf{M}}})$			Time for $\tilde{\mathbf{M}}\mathbf{E}$ $(T_{\tilde{\mathbf{M}}\mathbf{E}})$			Speedup $= T_J \big/ (T_{\tilde{\mathbf{M}}} + T_{\tilde{\mathbf{M}}\mathbf{E}})$		
	n	$\varepsilon = 10^{-3}$	10^{-4}	10^{-5}	$\varepsilon = 10^{-3}$	10^{-4}	10^{-5}	$\varepsilon = 10^{-3}$	10^{-4}	10^{-5}
City 1	8897	0.17s	0.68s	2.51s	0.52s	1.22s	2.88s	47.5 ×	27.2 ×	14.8 ×
	35588	1.10s	7.08s	32.80s	3.72s	10.20s	26.70s	69.4 ×	34.4 ×	16.7 ×
	142352	7.33s	60.90s	440.00s	26.40s	89.80s	264.00s	110.0 ×	43.9 ×	20.1 ×
City 2	8897	0.26s	1.49s	5.80s	0.71s	1.99s	4.99s	45.2 ×	22.0 ×	10.9 ×
	35588	2.06s	15.20s	79.60s	5.17s	16.20s	45.70s	73.4 ×	30.7 ×	13.5 ×
	142352	11.80s	136.00s	1180.00s	34.20s	140.00s	442.00s	124.0 ×	41.7 ×	16.9 ×
City 3	8897	0.52s	4.10s	18.40s	1.09s	4.04s	11.90s	45.3 ×	15.9 ×	6.7 ×
	35588	3.35s	38.00s	264.00s	6.91s	29.10s	100.00s	80.6 ×	26.2 ×	9.3 ×
	142352	15.80s	306.00s	4070.00s	37.70s	223.00s	837.00s	188.0 ×	42.2 ×	14.7 ×

Table 2: Execution times (in seconds) of radiosity calculations for the test cases.

4.4 Radiosity Results

In this section we study the impact of the proposed algorithm on the radiosity results. We use 132 different sky configurations, each one with a unique sky element illuminating the scene, to compute 132 radiosity solutions of the city. Given a patch of the city, the radiosity value

calculated for each of the sky configurations is related to the concept of Daylight Coefficient ([Tregenza and Waters, 1983]). The linear combinations of the radiosity solutions for the 132 skies allow to find the radiosity of the city for any other sky configuration. Fig. 2 shows the radiosity values of the three cities for the same sky configuration, when ε=10^{-5}.

Comparison with Jacobi

Table 3 shows the relative errors of the 132 radiosities obtained, comparing $\widetilde{B} = \widetilde{\mathbf{M}}E$ to the solution (B_J) of the Jacobi iteration methodology (Eq. 2). The initial emission is the first bounce of the light emitted from the sky (Sec. 3.3). The mean, standard deviation and maximum values are reported. As expected, the error gets smaller as the city homogeneity increases and as the truncation factor decreases. For every case, the standard deviation is small, as well as the maximum error is close to the mean value.

		Relative error of $\widetilde{B}$: $\frac{\|\widetilde{B}-B_J\|}{\|B_J\|}$ ($\times$1000)								
		$\varepsilon = 10^{-3}$			$\varepsilon = 10^{-4}$			$\varepsilon = 10^{-5}$		
	n	μ	σ	Max	μ	σ	Max	μ	σ	Max
City 1	8897	27.80	2.29	29.40	7.83	0.73	8.29	1.88	0.19	2.00
	35588	53.00	3.17	55.70	16.90	1.25	17.90	4.53	0.36	4.78
	142352	48.60	5.09	52.80	15.30	1.88	16.70	4.15	0.57	4.57
City 2	8897	87.70	6.44	95.20	31.70	2.99	34.20	9.50	1.04	10.30
	35588	86.50	9.15	97.80	35.00	5.42	39.80	11.00	2.20	12.80
	142352	134.00	11.70	154.00	61.80	6.24	69.30	23.00	3.41	25.90
City 3	8897	92.60	3.92	98.20	33.30	2.11	35.30	9.86	0.72	10.50
	35588	141.00	8.67	155.00	59.30	4.80	64.20	19.70	1.93	21.40
	142352	189.67	17.74	221.03	99.20	8.45	113.05	42.14	4.77	47.12

Table 3: Radiosity errors for the test cases (all numbers are $\times$1000).

Radiosity 3^{rd} and successive bounces

In Fig. 4, the average radiosity values for the 132 different sky configurations are shown (for two city models). All the radiosity curves are sorted from lowest to highest values. In both plots, we present the results using the Jacobi iteration method for computing radiosity (B_J) and only the third and successive bounces (S_J). Also, we show the same results using the proposed algorithm for different truncation thresholds.

As can be appreciated, the illumination is much higher in B_J than in S_J, because the first two bounces are the main component of the total radiosity. Nevertheless, the rest of the bounces together are not negligible, which means that they cannot be discarded in the calculations. Taking a closer look into the results of the proposed algorithm, it is evident that a higher truncation threshold implies a higher error. When compared to the Jacobi solution, the results seem close enough for most practical applications, when ε=10^{-4} and 10^{-5}. Finally, the errors on the third and successive bounces seem uniform.

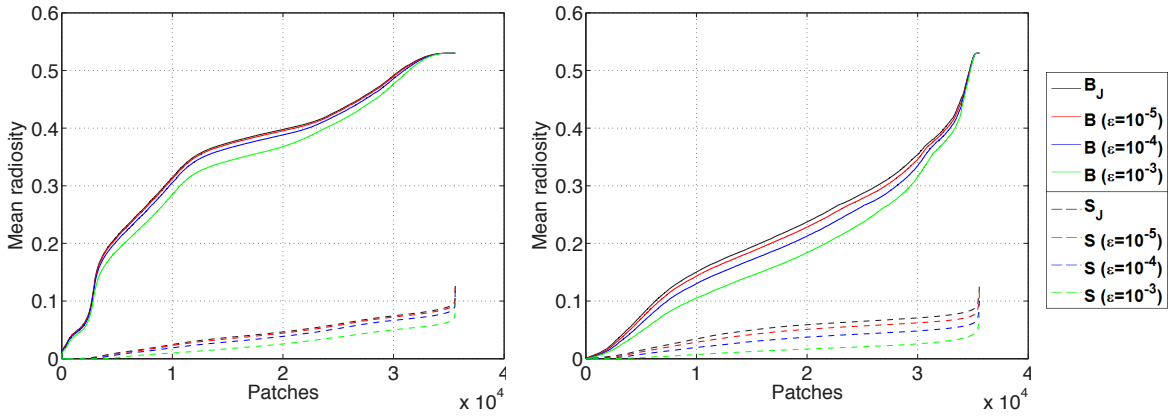

(a) City 1. (b) City 3.

Figure 4: Comparison of radiosity results between Jacobi ($\mathbf{B}_j$), third and successive bounces ($\mathbf{S}_j$), and their approximations using different thresholds.

5 Conclusions and Future Work

This work is a first step into the study of the correlation between the characteristics of a city and the sparsity of its form factors matrix ($\mathbf{F}$). Here we focus on the variation of building heights. We studied three different cities, and found that more homogeneous cities produce more sparse $\mathbf{F}$ matrices. The matrices are sparse enough to be stored in the main memory of a desktop computer, considering city scenes that contain up to 140k patches. Another result is the calculation of a sparse approximation to the inverse of the radiosity matrix ($\tilde{\mathbf{M}}$). This approximation is based on the use of Neumann series and the elimination of all terms with lower values than a given threshold. $\tilde{\mathbf{M}}$ is also sufficiently sparse as to be stored in main memory. These matrices were tested doing radiosity calculations for several sky configurations. We compared the results with a Jacobi iteration method, and found that the radiosities have low relative errors. Additionally, the proposed method is time efficient.

Further works should address the study of $\mathbf{F}$ for real cities, and also to take other characteristics into account. The calculation of $\tilde{\mathbf{M}}$ could allow the use of standard skies and meteorological yearly data, to perform statistical analyses related to the use of natural light in cities. These results can have a big influence into the definition of city regulations. Other possible line of work is related to the design of new city elements, like buildings and public places, taking into consideration the main characteristics of the surroundings. Finally, to apply the proposed methods to thermal radiation and heat accumulation on urban environments, we should consider the main aspects related to the heat equation.

Acknowledgments

The work was partially supported by FSE_1_2014_1_102344 project from Agencia Nacional de Investigación e Innovación (ANII, Uruguay) and TIN2014-52211-C2-2-R project from Ministerio de Economía y Competitividad, Spain.

References

[Baker and Steemers, 2014] Baker, N. and Steemers, K. (2014). *Daylight design of buildings: A handbook for architects and engineers*. Routledge.

[Beckers, 2013a] Beckers, B. (2013a). *Solar energy at urban scale*. John Wiley & Sons.

[Beckers, 2013b] Beckers, B. (2013b). Taking advantage of low radiative coupling in 3d urban models. In *Proceedings of the Eurographics Workshop on Urban Data Modelling and Visualisation*, pages 17–20. Eurographics Association.

[Borel et al., 1991] Borel, C. C., Gerstl, S. A., and Powers, B. J. (1991). The radiosity method in optical remote sensing of structured 3-d surfaces. *Remote Sensing of Environment*, 36(1):13–44.

[Chelle and Andrieu, 1998] Chelle, M. and Andrieu, B. (1998). The nested radiosity model for the distribution of light within plant canopies. *Ecological Modelling*, 111(1):75–91.

[Cohen and Greenberg, 1985] Cohen, M. F. and Greenberg, D. P. (1985). The hemi-cube: A radiosity solution for complex environments. In *ACM SIGGRAPH Computer Graphics*, volume 19, pages 31–40. ACM.

[Cohen and Wallace, 2012] Cohen, M. F. and Wallace, J. R. (2012). *Radiosity and realistic image synthesis*. Elsevier.

[Dutre et al., 2006] Dutre, P., Bala, K., Bekaert, P., and Shirley, P. (2006). *Advanced Global Illumination*. AK Peters Ltd.

[Fernández, 2009] Fernández, E. (2009). Low-rank radiosity. In *Proceedings of the IV Iberoamerican symposium in computer graphics. Sociedad Venezolana de Computación Gráfica*, pages 55–62.

[Goel et al., 1991] Goel, N. S., Rozehnal, I., and Thompson, R. L. (1991). A computer graphics based model for scattering from objects of arbitrary shapes in the optical region. *Remote Sensing of Environment*, 36(2):73–104.

[Goral et al., 1984] Goral, C. M., Torrance, K. E., Greenberg, D. P., and Battaile, B. (1984). Modeling the interaction of light between diffuse surfaces. In *Proceedings of the 11th annual conference on Computer graphics and interactive techniques*, SIGGRAPH '84, pages 213–222, New York, NY, USA. ACM.

[Gortler et al., 1993] Gortler, S. J., Schröder, P., Cohen, M. F., and Hanrahan, P. (1993). Wavelet radiosity. In *Proceedings of the 20th annual conference on Computer graphics and interactive techniques*, pages 221–230. ACM.

[Hviid et al., 2008] Hviid, C. A., Nielsen, T. R., and Svendsen, S. (2008). Simple tool to evaluate the impact of daylight on building energy consumption. *Solar Energy*, 82(9):787–798.

[Kirk and Hwu, 2010] Kirk, D. B. and Hwu, W.-m. W. (2010). *Programming Massively Parallel Processors: A Hands-on Approach*. Morgan Kaufmann Publishers Inc., San Francisco, CA, USA, 1st edition.

[Kontkanen et al., 2006] Kontkanen, J., Turquin, E., Holzschuch, N., and Sillion, F. X. (2006). Wavelet radiance transport for interactive indirect lighting. In *Rendering Techniques 2006 (Eurographics Symposium on Rendering)*, pages 161–171.

[Longcore and Rich, 2004] Longcore, T. and Rich, C. (2004). Ecological light pollution. *Frontiers in Ecology and the Environment*, 2(4):191–198.

[Mardaljevic, 1999] Mardaljevic, J. (1999). *Daylight simulation: validation, sky models and daylight coefficients*. De Montfort University.

[MATLAB, 2010] MATLAB (2010). *version 7.10*. The MathWorks Inc., Natick, Massachusetts.

[Robinson et al., 2009] Robinson, D., Haldi, F., Kämpf, J., Leroux, P., Perez, D., Rasheed, A., and Wilke, U. (2009). CitySim: Comprehensive micro-simulation of resource flows for sustainable urban planning. In *Proc. Building Simulation*.

[Robinson and Stone, 2005] Robinson, D. and Stone, A. (2005). A simplified radiosity algorithm for general urban radiation exchange. *Building Services Engineering Research and Technology*, 26(4):271–284.

[Tregenza, 1987] Tregenza, P. (1987). Subdivision of the sky hemisphere for luminance measurements. *Lighting Research and Technology*, 19(1):13–14.

[Tregenza and Waters, 1983] Tregenza, P. and Waters, I. (1983). Daylight coefficients. *Lighting Research and Technology*, 15(2):65–71.

[Wilkinson, 1971] Wilkinson, J. (1971). The algebraic eigenvalue problem. In *Handbook for Automatic Computation, Volume II, Linear Algebra*. Springer-Verlag New York.